Enhanced Fluorescence of Gold Nanoclusters Composed of $HAuCl_4$ and Histidine by Glutathione: Glutathione Detection and Selective Cancer Cell Imaging

Xiaodong Zhang, Fu-Gen Wu, Peidang Liu, Ning Gu, and Zhan Chen**

Glutathione (GSH) can significantly and selectively enhance the fluorescence intensity of Au nanoclusters (NCs) prepared by blending $HAuCl_4$ and histidine in solution. The quantum yield of the Au NCs after adding GSH can reach above 10%. Besides, GSH capping shifts the excitation peak of Au NCs from ultraviolet (386 nm) to visible light (414 nm) and improves the stability of the Au NCs. The cytotoxicities of the Au NCs with and without GSH for normal lung cells (ATII) and cancerous lung cells (A549) are evaluated. The GSH-capped Au NCs have much less cytotoxicity to both normal and cancer cells, as compared to those without GSH. For Au NCs without GSH, less cytotoxicity is observed in cancer cells than in normal cells. In addtion, the Au NCs can selectively detect GSH over cysteine and homocysteine, the two biothiols which commonly exist in cells that can seriously affect GSH detection. Most importantly, Au NCs without GSH can selectively image the cancer cells, especially for the liver cancer cells whose GSH content is much higher than other cell types. This property makes the Au NCs a powerful probe to distinguish cancer cells from normal cells.

1. Introduction

Glutathione (GSH) is an important antioxidant and the most abundant low-molecular thiol in vivo with a concentration range from 1 to 15 mM.[1] GSH can prevent damage to important cellular components caused by reactive oxygen species (ROS) such as free radicals and peroxides.[2] GSH participates in many physiological processes including xenobiotic metabolism, intracellular signal transduction, and gene regulation. Moreover, GSH also involves in regulating cancer cell death, including apoptosis, necrosis, and autophagy.[3] Increased levels of GSH and the resulting resistance to chemotherapeutic agents (e.g., doxorubicin and platinum containing compounds) in cancer cells have been observed.[4] Due to the importance of GSH, it is desired to develop a highly selective and quantitative method to detect GSH.

A number of analytical methods based on fluorescence were developed due to its superb selectivity and high sensitivity. The fluorescence instrumentation is also very simple and the detection method is nondestructive to the sample under study. Yang and co-workers designed a ratiometric, monochlorinated BODIPY-based fluorescence sensor to detect GSH and it can be used in living cells.[5] Yoon et al. successfully prepared two cyanine-based fluorescent probes to detect GSH in cell culture and live mouse tissue.[6] In addition to organic dyes used in the fluorescence detection, quantum dots have also been used to detect GSH. Sensitive

X. D. Zhang, Prof. F.-G. Wu, Prof. P. D. Liu, Prof. N. Gu
State Key Laboratory of Bioelectronics, School of Biological Science and Medical Engineering
Southeast University
Nanjing 210096, China
E-mail: wufg@seu.edu.cn
Prof. Z. Chen
Department of Chemistry
University of Michigan
930 North University Avenue, Ann Arbor, Michigan 48109, USA
E-mail: zhanc@umich.edu
Prof. P. D. Liu
School of Medicine
Southeast University
Nanjing 210009, China

DOI: 10.1002/smll.201401658

small NANO MICRO

turn-on fluorescence sensors to detect GSH in cells based on the recovered fluorescence of "Au NC–Hg^{II}"[7] and "CdTe/CdSe quantum dot–Hg^{II}"[8] have been developed.

On the other hand, gold nanoclusters (Au NCs) composed of several to a hundred gold atoms with a typical size of 1–5 nm are an important class of fluorescent nanostructures that can also be used to detect GSH in vitro and in vivo. Like other gold-based nanomaterials that have various applications owning to their excellent biocompatibility,[9] Au NCs bearing unique physicochemical properties[10] are also safe and can be used for molecular identification[7,11] and ion detection,[12] catalysis,[13] and potential applications in biolabeling and sensing.[14] Au NCs can be synthesized by using different capping molecules, such as peptides,[15] proteins,[16] DNA,[17] polymers[18] including PAMAM,[19] adenine and its derivatives,[20] histidine,[21] GSH,[12c,15c,22] purine,[23] dihydrolipoic acid,[12b] diphospine,[24] and alkanethiol.[25] Among these capping reagents, GSH is considered to be excellent due to its superb biocompatibility and stability.[12c,15c,22]

Herein, we report for the first time that by adding GSH, the fluorescence intensity of Au NCs prepared by blending $HAuCl_4$ and histidine can be significantly, selectively, and linearly enhanced. The preparation and characterization of the Au NCs made from $HAuCl_4$ and histidine has already been reported by Chen et al.[21a] We found that the thus-prepared Au NCs shows a superb ability to selectively detect GSH over cysteine (Cys) and homocysteine (Hcy), the two biothiols commonly exist in cells that can seriously affect GSH detection. It was also found that the Au NCs without GSH can selectively distinguish cancer cells (e.g., lung A549 and liver Hep G2 cancer cells) from normal cells (e.g., lung ATII and liver L02 cells), based on the different GSH concentrations of the two types of cells. Au NCs were shown to be able to cause a much stronger fluorescence enhancement in liver cancer cells (Hep G2 cells) than in lung cancer cells (A549 cells). Besides, cytotoxicity evaluations of the Au NCs with and without GSH were also carried out for normal lung cells (ATII) and cancerous lung cells (A549).

2. Results and Discussion

The TEM image of the Au NCs revealed no apparent difference in morphology between the Au NCs containing GSH and those without GSH (see supporting information Figure S1). However, the GSH-containing Au NCs can be stable for more than two weeks, which is much longer than the Au NCs without GSH (which will precipitate after storage for 1 or 2 days). We collected the UV-Vis absorption spectrum from the Au NCs with GSH (e.g., at a GSH:Au ratio of 12:1) between 300 nm and 700 nm (**Figure 1**A). There was no absorption detected for the wavelength region > 600 nm. Absorption was observed between 300 nm and 600 nm, with a small peak centered near 414 nm. The fluorescent spectra also indicated that the maximum excitation peak centered at 414 nm, a significant shift from that of the Au NCs without GSH (384 nm).[21a] Under the 414 nm excitation, the sample generated a fluorescence emission peak at about 496 nm (Figure 1A). Using quinine sulfate as the reference, the quantum yield is estimated to be about 10% for GSH: Au NCs = 24:1. Further increasing

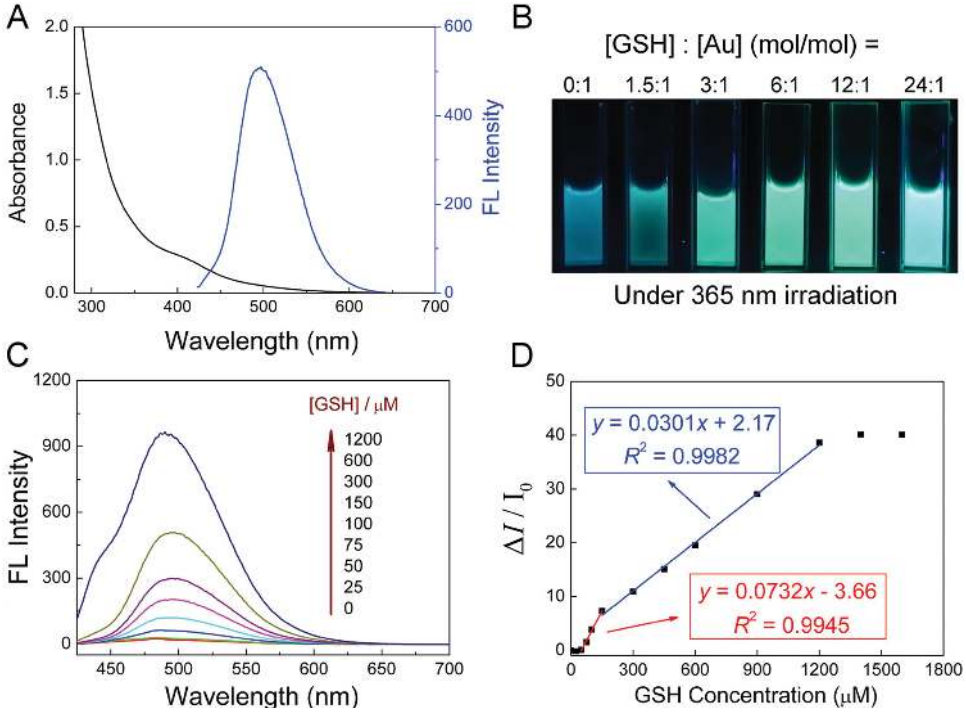

Figure 1. (A) UV-Vis absorption spectrum (left) and emission spectrum excited at 414 nm (right) of GSH : Au NCs = 12 : 1 (mol/mol); (B) Photographs of GSH mixing with Au NCs using different molar ratios: 0 : 1, 1 : 1, 1.5 : 1, 3 : 1, 6 : 1, 12 : 1, and 24 : 1 (from left to right) under 365 nm UV excitations; (C) Fluorescence responses of 50 μM Au NCs after adding GSH to reach different concentrations (0–1200 μM); (D) Plot of the relationship between $\Delta I/I_0$ and [GSH] (0–1600 μM).

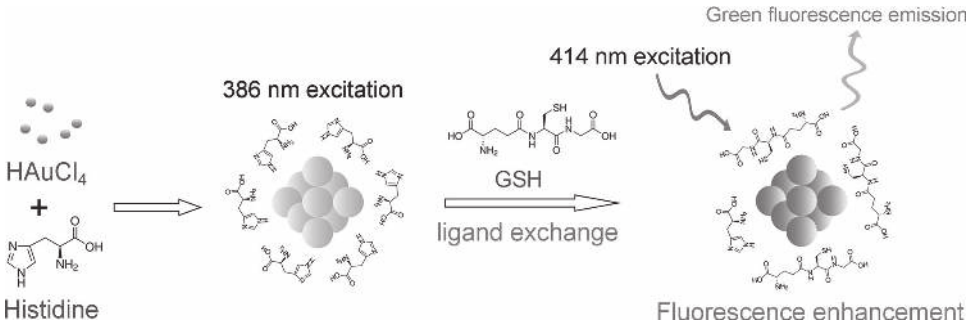

Scheme 1. Schematics illustrating the GSH-induced fluorescence enhancement of Au NCs prepared by mixing $HAuCl_4$ and histidine.

the content of GSH can increase the quantum yield of Au NCs to above 10%. **Scheme 1** illustrates the general process of the GSH-induced fluorescence enhancement of Au NCs.

The fluorescence intensity of Au NCs increased after adding different concentrations of GSH under the 365 nm UV irradiation (Figure 1B). The fluorescence enhancement of Au NCs by different concentrations of GSH was also shown in the fluorescence spectra (Figure 1C). As the concentration of GSH increased, the fluorescence intensity of Au NCs was monotonically enhanced. Figure 1D showed the change of fluorescence intensity ($\Delta I/I_0$) at 496 nm as a function of GSH concentration ([GSH]). The $\Delta I/I_0$ values were measured over the GSH concentration range of 50–1600 μM. The dependence of $\Delta I/I_0$ on GSH concentration follows two equations in two concentration ranges: $\Delta I/I_0 = -3.66 + 0.0732 \times [GSH]$ ($R^2 = 0.9945$) from GSH concentration of 50 μM to 150 μM and $\Delta I/I_0 = 2.17 + 0.0301 \times [GSH]$ ($R^2 = 0.9982$) from GSH concentration of 150 to 1200 μM, with a detection limit of 0.2 μM (at a signal to noise ratio of 3), respectively. As a result of the strong Au–S bond, the added GSH (a thiol-containing short peptide) can gradually have a ligand exchange with the previous histidine molecules on the surface of Au NCs, leading to a significant fluorescence enhancement of the Au NCs. We can also fit the data (from 50 to 1200 μM) using one equation $\Delta I/I_0 = 0.323 + 0.0322 \times [GSH]$ ($R^2 = 0.9905$). However, such a simple one-equation fitting cannot accurately reflect the [GSH]-dependent fluorescent intensity changes, especially at low GSH concentrations. The different fluorescence responses in two concentrations ranges may indicate that there are two stages of GSH interactions with Au NCs. We believe that the fluorescent signal increase after the addition of GSH is due to the ligand exchange between GSH and histidine. At high GSH concentrations, the increase of GSH in the solution may not as effectively replace the original histidine ligands on the surface of the Au NCs as in the low [GSH] situation, because the Au NC surface already has substantial GSH coverage. We also find that the fluorescence intensity changes of a higher GSH:Au ratio of 28:1 ([GSH] = 1400 μM) and 32:1 ([GSH] = 1600 μM) deviate from the linear relationship (Figure 1D).

The ligand exchange between histidine and GSH on the surface of Au NCs can be verified by XPS. The XPS spectrum of the GSH-capped Au NCs shows the binding energies of all the elements in the product (Figure S2). Specifically, the elements of C, N, O, and S were detected from Au NCs with histidine and GSH. The presence of the S 2p peak at 162.3 eV indicates the interaction of Au NCs with GSH through the Au–S bond. The binding energy of Au 4f7/2 shifts from 83.9 eV to 82.8 eV after the addition of GSH (**Figure 2**A), indicating a reduction of partial Au(I) atoms to Au(0) atoms in Au NCs by GSH molecules. The XPS data indicate the strong interaction between GSH and Au NCs.

The fluorescence lifetimes of the Au NCs before and after addition of GSH were also measured to study the effect of GSH on the fluorescence properties (Figure 2B). The decay curve of Au NCs without GSH can be fitted with a double exponential function, giving two distinct decay times of 1.58 and 5.56 ns, respectively. This may imply that there are two

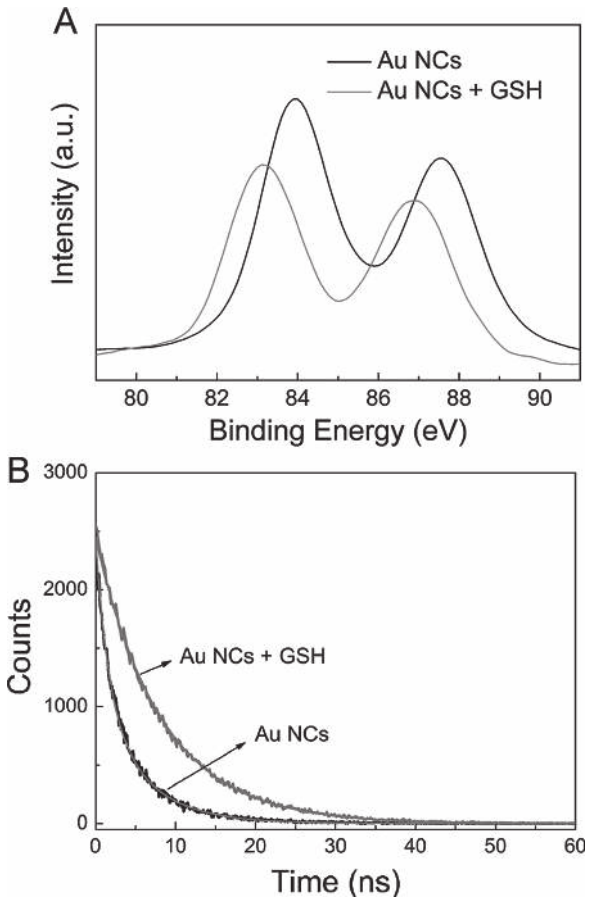

Figure 2. (A) XPS spectra of Au 4f for Au NC (black line) and GSH-capped Au NCs (grey line); (B) Time-resolved fluorescence decay curves of Au NCs and GSH-capped Au NCs.

small NANO MICRO

competing fast and slow electron transfer processes. After adding GSH, the decay curve of Au NCs can be fitted with a single exponential function, giving a decay time of 8.29 ns. The longer lifetime of Au NCs after the addition of GSH implied that GSH (which was bound to the surface of Au NCs) acted as an electron donor to enhance the fluorescence of Au NCs.[26]

Since the Au NCs will be used for detecting GSH, we also studied the possible fluorescence enhancement effect of Au NCs caused by other common molecules in the cell medium. As shown in **Figure 3**, the fluorescence intensity of the Au NCs exhibited a significant enhancement by adding GSH to the solution, whereas other molecules such as amino acids including L-glutamic acid (Glu), glycine (Gly), D,L-homocysteine (Hcy), L-serine (Ser), L-arginine (Arg), L-lysine (Lys), L-cysteine (Cys), and L-glutamine (Gln), small molecules (including DTT and glucose) and ions (including K^+, Na^+, and Ca^{2+}) did not cause similar obvious fluorescence changes compared to GSH. Figure 3 shows that the Au NCs can sensitively distinguish GSH from Hcy and Cys. Hcy and Cys are also thiol-containing molecules and involved in many physiological processes, especially in the cellular antioxidant defense system. Hcy is an important marker for cardiovascular disease[27] and osteoporotic fracture.[28] While as a precursor to GSH, Cys is an important source of sulfide in human metabolism and plays an important role in influencing protein structure.[29] Therefore Hcy and Cys are widely available in the cell medium. Here we clearly demonstrated that Hcy and Cys will not interfere with the detection of high concentration of GSH using Au NCs.

Two possible reasons may explain why other thiol-containing molecules (such as DTT, Hcy, and Cys) cannot significantly enhance the fluorescence intensity of Au NCs like GSH. The fluorescence enhancement may be attributed to the so-called "charge transfer from the ligands to the metal center (LMNCT)" mechanism through the Au–S bonds. The LMNCT mechanism has been widely used to explain the luminescence and luminescent enhancement of noble metal nanoclusters protected by thiol ligands, such as alkanethiol and glutathione.[30] In the case of Au NCs, the formation of the Au–S bond after the addition of thiol compound implied

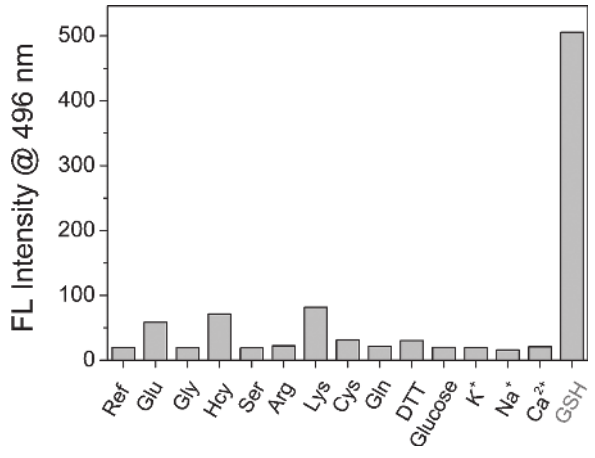

Figure 3. Fluorescence responses of 50 μM Au NCs with different guest molecules. The concentrations of all guests are 600 μM.

that the charge transfer might occur between the Au NCs and the thiol compound. Compared with Hcy and Cys, GSH contains more electron-rich groups, such as carboxyl group (COOH) and amino group (NH_2), which might also contribute to the fluorescence enhancement.[31] Another possible explanation is the large steric hindrance effect created by GSH (larger than DTT, Hcy, and Cys), which enhances the coordination stability to metal atoms.[7,8] The stable structure may also lead to the significant fluorescence enhancement.

We have tested the fluorescence intensity of the Au NCs when GSH, Hcy, and Cys are coexisted. Compared to the fluorescence intensity generated from Au NCs blending only with GSH (Au:GSH = 1:12, mol/mol), the fluorescence intensity of Au NCs mixing with GSH, Hcy, and Cys (Au:GSH:Hcy:Cys = 1:12:12:12, mol/mol/mol/mol) decreased by ~40% after incubation for 12 h. This demonstrates that the two other thiol-containing molecules (Hcy and Cys) may compete with GSH to interact with Au NCs. As we observed and explained above, the enhancement effect of GSH is larger than Hcy and Cys, therefore when GSH, Hcy and Cys are coexisted, the Au NC florescence intensity is weaker than the case when GSH is present alone. In certain cells and tissues, the content of GSH is higher than those of Hcy and Cys, and thus the competing effect of Hcy and Cys will not significantly affect the GSH-induced fluorescence enhancement.

We have also tested if GSH can enhance the fluorescence intensity of Au NCs prepared using other methods, e.g., by mixing $HAuCl_4$ and BSA.[16a] The results shown in the Figure S3 indicated that the fluorescence intensity of Au NCs could also be significantly enhanced by the presence of GSH, which suggested that the GSH-caused fluorescence enhancement should be a general phenomenon for Au NCs.

In comparison to other fluorescence probes, the Au NCs probe has three advantages. First of all, the system is "clean" and there are no other heavy metals (besides gold) in the system. Previous studies detected GSH using fluorescence quenching of Au NCs with heavy metal ions (such as mercury ion) and recovery of the fluorescence as a result of the preferable affinity of GSH with heavy metal ions.[7,8] Most heavy metals are toxic and their accumulation over time in the body can cause serious illness. Thus, here we developed a much safer method to detect GSH in living cells. Secondly, the current probe is easy to prepare, simply by blending $HAuCl_4$ and histidine in solution at room temperature. No organic synthesis, redox reaction, separation or purification steps are needed in the entire experimental procedures. Moreover, the system has a specific sensitivity and high selectivity to detect GSH. The interference of other possible coexisting substances in cell medium is low, especially for those biothiols with similar structures and reactivities (e.g., Hcy and Cys). Previously because both of the two thiol-containing molecules Hcy and Cys strongly interfered with GSH detection,[32] the GSH detection has significant challenges.[33]

MTT assay experiments showed that the Au NCs (without GSH) are more toxic to normal ATII cells (**Figure 4**A) than cancerous A549 cells (Figure 4B). For example, after the addition of 300 μM Au NCs to both types of the cells, the measured cell viabilities for A549 and ATII cells are ~82% and ~33%, respectively. After adding the GSH-capped

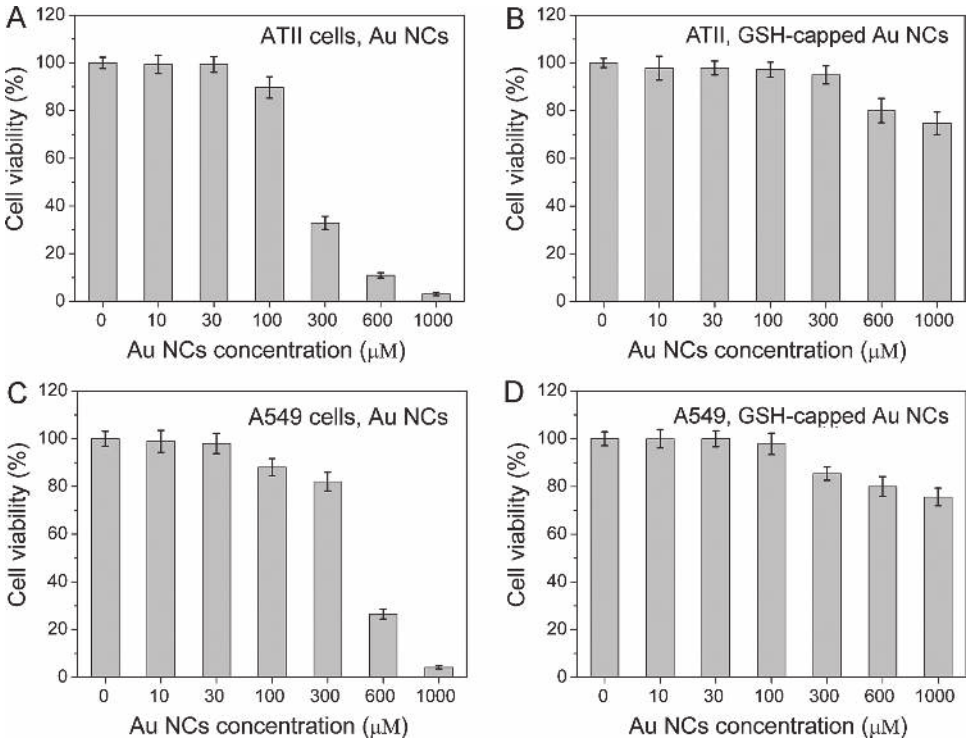

Figure 4. Cytotoxicity results of Au NCs and GSH-capped Au NCs (with the GSH/Au molar ratio of 12 : 1) on ATII (A and B) and A549 cells (C and D) determined by MTT assay.

Au NCs, the cytotoxicity of Au NCs to ATII (Figure 4C) and A549 (Figure 4D) cells significantly decreased. It was observed that at the highest concentration of 1000 μM GSH-capped Au NCs, the cell viability values of ATII and A549 cells are still measured to be ~75% and ~76%, respectively. In contrast, after adding 1000 μM Au NCs (without GSH), the cell viability values of ATII and A549 cells are only ~3% and ~4%, respectively. This indicates that the incorporation of GSH to Au NCs can significantly protect both normal cells and cancer cells. This can in turn explain the result that the cancerous A549 cells are more resistant to Au NCs compared with normal ATII cells, since the cancer cells have a higher content of GSH relative to normal cells. As an effective antioxidant, GSH can prevent damage of important cellular components caused by reactive oxygen species (ROS), which shows that the predominant reason for the cytotoxicity of Au NCs at concentrations higher than 100 μM is the production of ROS within cells after exposure to Au NCs. However, the above MTT assay results show that the two kinds of Au NCs (with or without GSH) are not toxic to either normal cells or cancer cells at concentrations of 100 μM or below, which makes the Au NCs suitable for other applications such as cell imaging.

To demonstrate if the Au NCs have the ability to selectively image cancer cells, we chose two kinds of human cell lines, the liver cells (including normal L02 cells and cancerous Hep G2 cells) and lung cells (including normal ATII cells and cancerous A549 cells), and used confocal microscopy to study the imaging effects of the Au NCs prepared by $HAuCl_4$ and histidine. ATII cells have a very weak autofluorescence intensity, and the results in **Figure 5**A and C show that the addition of 100 μM Au NCs to ATII cells did not cause noticable change in the fluorescence intensity of the cells. For A549 cells, the addition of 100 μM Au NCs resulted in the formation of some bright fluorescence dots within the cells (Figure 5D and Figure S4), whose fluorescence intensity is much higher as compared to the autofluorescence intensity of the A549 cells (Figure 5B). Such a fluorescence dot

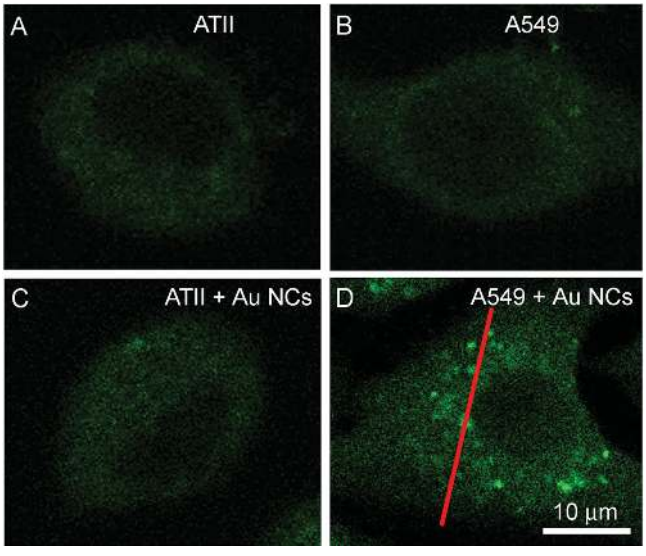

Figure 5. Confocal fluorescence images of (A) ATII cells without Au NCs, (B) A549 cells without Au NCs, (C) ATII cells with 100 μM Au NCs and (D) A549 cells with 100 μM Au NCs. Cell images were obtained using an excitation wavelength of 405 nm. The fluorescence intensity in the area along the line marked in (D) will be quantified in Figure 7A below.

small NANO MICRO

formation character is more pronounced in cancerous liver cell lines after the addition of Au NCs (**Figure 6**). After adding 100 μM Au NCs to L02 cells, there was no apparent fluorescence intensity change before (Figure 6A) and after the addition of Au NCs (Figure 6C). While for Hep G2 cells, intense green fluorescence dots appeared within the cytoplasm of the cells after the addition of Au NCs (Figure 6D). The fluorescence enhancement in the two cancerous cells may be related to the elevated GSH concentrations in cancer cells as compared to the corresponding normal cells. Besides, it has been reported that the content of GSH in liver is about 4–7 times higher than that in lung, heart, and brain,[34] which may account for the observed more evident fluorescent dot formation in cancerous liver cells. Our present work shows that the Au NCs prepared from $HAuCl_4$ and histidine can be used as an excellent sensor for GSH within living cells, and can selectively image cancer cells, especially for liver cancer cells.

To quantify the occurrence frequency of the fluorescent dots within A549 and Hep G2 cells after the addition of Au NCs, we measured the fluorescence intensities in the areas along the straight lines marked in the confocal images in Figure 5D and Figure 6D and showed the results in **Figure 7**A,B. Under the same 405 nm excitation, the fluorescence intensities of the two samples are similar. However, the occurrence frequency of the fluorescent dots in the "Hep G2 + Au NCs" sample is much higher than that in the "A549 + Au NCs" sample. Besides, the fluorescence intensities of Au NCs in each cell were obtained by calculating the integrated intensity of the cell divided by the cell area (Figure 7C). The results also showed that the integrated fluorescence intensity in Hep G2 cells after the addition of Au NCs was larger than that in A549 cells.

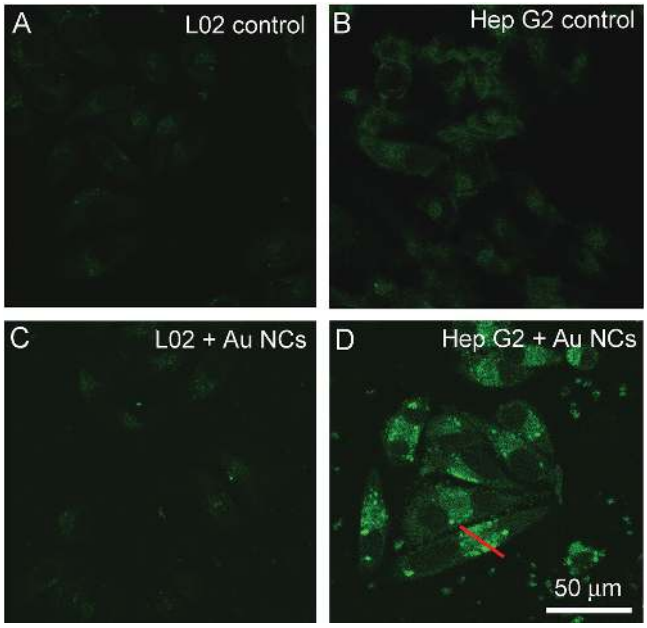

Figure 6. Confocal images of (A) L02 cells without Au NCs, (B) Hep G2 cells without Au NCs, (C) L02 cells with 100 μM Au NCs and (D) Hep G2 cells with 100 μM Au NCs. Cell images were obtained using an excitation wavelength of 405 nm. The fluorescence intensity in the area along the line marked in (D) will be quantified in Figure 7B below.

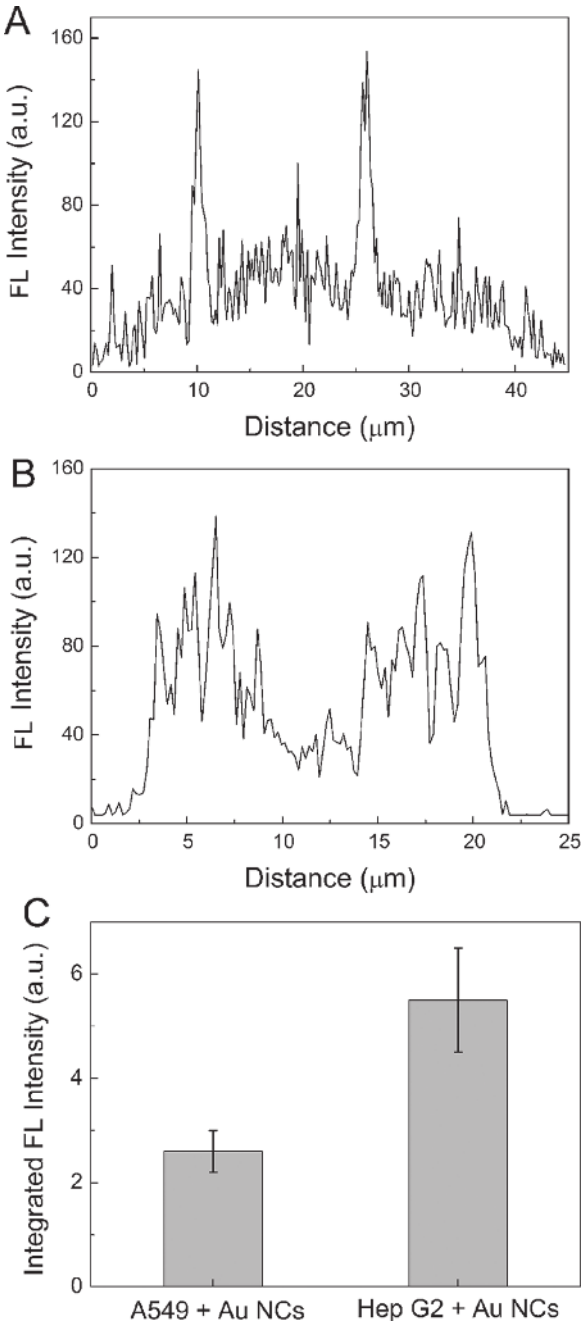

Figure 7. Fluorescence intensities of the red lines marked in the confocal images for (A) A549 + Au NCs (Figure 5D) and (B) Hep G2 + Au NCs (Figure 6D). (C) Integrated fluorescence intensity of A549 (Figure S4) and Hep G2 (Figure 6D) cells after incubation with Au NCs for 24 h.

GSH reduces disulfide bonds within cytoplasmic proteins to thiols while being oxidized to GSSG and can be regenerated from GSSG by the enzyme glutathione reductase. In healthy cells and tissues, more than 90% of the total glutathione exists in the reduced form (GSH) and an increased GSSG-to-GSH ratio is considered to be indicative of oxidative stress.[35] The ROS stress in cancer cells is much greater than that in normal cells. As a result, more reduced glutathione (GSH) than oxidized glutathione (GSSG) is produced, which can have ligand exchange with the Au NCs,

producing enhanced fluorescent signals within the cancer cells. Our present work demonstrates that the Au NCs can effectively distinguish the cancer cells and normal cells by taking advantage of the GSH-enhanced mechanism of the Au NCs.

3. Conclusion

We have discovered that GSH can cause the fluorescence enhancement of Au NCs prepared by blending $HAuCl_4$ and histidine and protect both normal cells and cancer cells by reducing the cytotoxicity of the Au NCs. The quantum yield of the Au NCs after adding GSH can reach above 10%. Au NCs without GSH are more toxic to normal cells as compared to cancer cells due to the higher GSH concentration in cancer cells. The Au NCs without GSH can selectively image cancer cells, especially for liver cancer cells. Besides, the Au NCs prepared can efficiently detect GSH over cysteine (Cys), homocysteine (Hcy), and other common cell medium components.

4. Experimental Section

Materials: $HAuCl_4 \cdot 3H_2O$, L-histidine (His), L-glutathione (GSH), L-glutamic acid (Glu), L-arginine (Arg), L-lysine (Lys), L-serine (Ser), L-glutamine (Gln), L-cysteine (Cys), glycine (Gly), D,L-homocysteine (Hcy), dithiothreitol (DTT), glucose, KCl, NaCl, $CaCl_2$, and quinine sulfate were purchased from Sigma-Aldrich. All solutions were prepared with deionized water (18.2 MΩ·cm) purified by a Milli-Q system (Millipore).

Synthesis of Au NCs: All glassware was cleaned in a bath of freshly prepared aqua regia ($HCl:HNO_3$, 3:1 v/v) and rinsed thoroughly in Milli-Q water prior to use. An aqueous solution of histidine (15 mL, 0.1 M) was added to an aqueous solution of $HAuCl_4$ (5 mL, 10 mM) in a small vial at room temperature (about 25 °C). The solution mixture was blended gently at the beginning and then was placed at room temperature without stirring in dark for more than 3 h to prepare Au NC precursor solution. A series of GSH solutions were prepared with the concentrations varying from 0, 1.25, 2.5, 3.75, 5, 7.5, 15, 22.5, 30, 45, 60, 70, and 80 mM, respectively. An equal volume (1 mL) of the above-prepared GSH solution was then mixed with the above Au NC precursor solution to acquire a GSH:Au molar ratio of 0, 0.5, 1, 1.5, 2, 3, 6, 9, 12, 18, 24, 28, and 32. Afterwards, the mixtures were incubated without stirring in dark at room temperature overnight to prepare the final Au NCs.

Characterization of Au NCs: UV-Vis absorption spectra were recorded with a UV-2600 spectrophotometer (Shimadzu). Fluorescence spectra were collected on a RF-5301PC spectrofluorophotometer (Shimadzu) and an F-7000 fluorescence spectrophotometer (Hitachi). Transmission electron microscopic experiment (TEM) was performed on a JEM-2100 transmission electron microscope (JEOL). X-ray photoelectron spectroscopy (XPS) analysis was conducted by a PHI Quantera II X-ray photoelectron spectrometer (Ulvac-Phi). Fluorescence decay time measurement was obtained at 496 nm emission wavelength using 405 nm excitation on a FLS920 time-resolved fluorescence spectrometer (Edinburgh Instruments).

MTT Assay: To test the cytotoxicity of Au NCs in vitro, ATII and A549 cells were cultured in cell medium (DMEM), supplemented with 10% fetal bovine serum, 100 U of penicillin, and 100 mg/mL streptomycin in a humidified incubator at 37 °C and 5% CO_2. For the MTT toxicity test of Au NCs, the two cells were seeded in a 96-well plate in cell medium overnight and subsequently incubated with different concentrations of Au NCs (0, 10, 30, 100, 300, 600, and 1000 μM) in cell medium for 24 h at 37 °C and 5% CO_2. Afterwards, cell medium in each well was removed and each well was washed by PBS buffer. 100 μL cell medium containing 0.5 mg/mL MTT was added to each well. After incubation for 4 h at 37 °C and 5% CO_2, 150 μL DMSO was added to each well and mixed. The absorbance at 570 nm was measured with a Multiskan FC microplate photometer (Thermo).

Cell Imaging: L02 cells (normal liver cells), Hep G2 cells (cancerous liver cells), ATII cells (normal lung cells), and A549 cells (cancerous lung cells) were selected for using in this study. The cells were seeded in a Lab-Tek 8-well chambered coverglass (Nunc). After culturing for 24 h, 100 μM fresh Au NCs prepared by blending $HAuCl_4$ and histidine together were added to the cell medium. After incubation for another 24 h, the cells were washed with PBS and quickly observed under a confocal laser-scanning microscope (CLSM, Leica TCS-SP8) with an excitation wavelength of 405 nm. The confocal fluorescence images were quantitatively analyzed using the Image J software. The fluorescence intensity of Au NCs within each cell was obtained by calculating the integrated intensity divided by the cell area.

Supporting Information

Supporting Information is available from the Wiley Online Library or from the author.

Acknowledgements

This work was supported by grants from the National Key Basic Research Program of China (973 Program) (No. 2013CB933904), the Natural Science Foundation of China (21303017), the Natural Science Foundation of Jiangsu Province (KB20130601), and a project funded by the Priority Academic Program Development of Jiangsu Higher Education Institutions (1107037001). ZC thanks the University of Michigan to support his sabbatical.

[1] A. Pastore, F. Piemonte, M. Locatelli, A. Lo Russo, L. M. Gaeta, G. Tozzi, G. Federici, *Clin. Chem.* **2001**, *47*, 1467–1469.
[2] A. Pompella, A. Visvikis, A. Paolicchi, V. De Tata, A. F. Casini, *Biochem. Pharmacol.* **2003**, *66*, 1499–1503.
[3] a) A. L. Ortega, S. Mena, J. M. Estrela, *Cancers* **2011**, *3*, 1285–1310; b) Y. Chen, S. B. Gibson, *Autophagy* **2008**, *4*, 246–248.
[4] M. M. Gottesman, T. Fojo, S. E. Bates, *Nat. Rev. Cancer* **2002**, *2*, 48–58.
[5] L. Y. Niu, Y. S. Guan, Y. Z. Chen, L. Z. Wu, C. H. Tung, Q. Z. Yang, *J. Am. Chem. Soc.* **2012**, *134*, 18928–18931.
[6] J. Yun, Y. Kwon, D. Kim, D. Lee, G. Kim, Y. Hu, J. H. Ryu, J. Yoon, *J. Am. Chem. Soc.* **2014**, *136*, 5351–5358.

[7] D. H. Tian, Z. S. Qian, Y. S. Xia, C. Q. Zhu, *Langmuir* **2012**, *28*, 3945–3951.
[8] B. Y. Han, J. P. Yuan, E. K. Wang, *Anal. Chem.* **2009**, *81*, 5569–5573.
[9] a) J. Wang, G. Z. Zhu, M. X. You, M. B. O'Donoghue, M. I. Shukoor, K. J. Zhang, Y. Chen, Z. Zhu, E. Song, C. Z. Huang, W. H. Tan, *ACS Nano* **2012**, *6*, 5070–5077; b) J. Wang, M. X. You, G. Z. Zhu, M. I. Shukoor, C. M. Li, Z. Chen, Z. L. Zhao, M. B. Altman, Q. Yuan, Z. Zhu, Y. Chen, C. Z. Huang, W. H. Tan, *Small* **2013**, *9*, 3678–3684; c) J. N. Zhang, B. Liu, H. X. Liu, X. B. Zhang, W. H. Tan, *Nanomedicine* **2013**, *8*, 983–993.
[10] a) S. W. Chen, R. S. Ingram, M. J. Hostetler, J. J. Pietron, R. W. Murray, T. G. Schaaff, J. T. Khoury, M. M. Alvarez, R. L. Whetten, *Science* **1998**, *280*, 2098–2101; b) J. Zheng, P. R. Nicovichand, R. M. Dickson, *Annu. Rev. Phys. Chem.* **2007**, *58*, 409–431; c) K. A. Kacprzak, O. Lopez-Acevedo, H. Hakkinen, H. Gronbeck, *J. Phys. Chem. C* **2010**, *114*, 13571–13576; d) L. Shang, S. Dong, G. U. Nienhaus, *Nano Today* **2011**, *6*, 401–418.
[11] a) F. Wen, Y. H. Dong, L. Feng, S. Wang, S. C. Zhang, X. R. Zhang, *Anal.Chem.* **2011**, *83*, 1193–1196; b) H. Y. Liu, G. H. Yang, E. S. Abdel-Halim, J. J. Zhu, *Talanta* **2013**, *104*, 135–139; c) Y. Chen, Y. Y. Shen, D. Sun, H. Y. Zhang, D. B. Tian, J. R. Zhang, J. J. Zhu, *Chem. Commun.* **2011**, *47*, 11733–11735.
[12] a) C. C. Huang, Z. Yang, K. H. Lee, K. H. Lee, H. T. Chang, *Angew. Chem., Int. Ed.* **2007**, *119*, 6948–6952; b) L. Shang, L. X. Yang, F. Stockmar, R. Popescu, V. Trouillet, M. Bruns, D. Gerthsen, G. U. Nienhaus, *Nanoscale* **2012**, *4*, 4155–4160; c) H. Y. Zhang, Q. Liu, T. Wang, Z. Y. Yun, G. L. Li, J. Y. Liu, G. B. Jiang, *Anal. Chim. Acta* **2013**, *770*, 140–146; d) D. T. Lu, L. L. Liu, F. X. Liu, S. M. Shuang, Y. F. Li, M. M. F. Choi, C. Dong, *Spectrochim. Acta A* **2014**, *121*, 77–80.
[13] a) S. Yamazoe, K. Koyasu, T. Tsukuda, *Acc. Chem. Res.* **2014**, *47*, 816–824; b) L. Li, L. G. Dou, H. Zhang, *Nanoscale* **2014**, *6*, 3753–3763.
[14] a) C. A. J. Lin, T. Y. Yang, C. H. Lee, S. H. Huang, R. A. Sperling, M. Zanella, J. K. Li, J. L. Shen, H. H. Wang, H. I. Yeh, W. J. Parak, W. H. Chang, *ACS Nano* **2009**, *3*, 395–401; b) H. Y. Chen, S. L. Li, B. W. Li, X. Y. Ren, S. N. Li, D. M. Mahoungan, S. S. Cui, Y. Q. Gu, S. Achilefu, *Nanoscale* **2012**, *4*, 6050–6064; c) L. Shang, F. Stockmar, N. Azadfar, G. U. Nienhaus, *Angew. Chem., Int. Ed.* **2013**, *52*, 11154–11157; d) D. H. Hu, Z. H. Sheng, S. T. Fang, Y. N. Wang, D. Y. Gao, P. F. Zhang, P. Gong, Y. F. Ma, L. T. Cai, *Theranostics* **2014**, *4*, 142–153; e) K. Kwak, S. S. Kumar, K. Pyo, D. Lee, *ACS Nano* **2014**, *8*, 671–679; f) X. D. Zhang, J. Chen, Z. T. Luo, D. Wu, X. Shen, S. S. Song, Y. M. Sun, P. X. Liu, J. Zhao, S. D. Huo, S. J. Fan, F. Y. Fan, X. J. Liang, J. P. Xie, *Adv. Healthc. Mater.* **2014**, *3*, 133–141; g) R. Gui, A. Wan, X. Liu, H. Jin, *Chem. Commun.* **2014**, *50*, 1546–1548; h) H. Y. Liu, X. M. Wu, X. Zhang, C. Burda, J. J. Zhu, *J. Phys. Chem. C* **2012**, *116*, 2548–2554; i) J. W. Liu, *Trac-Trend Anal. Chem.* **2014**, *58*, 99–111.
[15] a) Y. Negishi, K. Nobusada, T. Tsukuda, *J. Am. Chem. Soc.* **2005**, *127*, 5261–5270; b) L. Fabris, S. Antonello, L. Armelao, R. L. Donkers, F. Polo, C. Toniolo, F. Maran, *J. Am. Chem. Soc.* **2006**, *128*, 326–336; c) X. Yuan, Z. T. Luo, Q. B. Zhang, X. H. Zhang, Y. G. Zheng, J. Y. Lee, J. P. Xie, *ACS Nano* **2011**, *5*, 8800–8808.
[16] a) J. P. Xie, Y. Zheng, J. Y. Ying, *J. Am. Chem. Soc.* **2009**, *131*, 888–889; b) X. Le Guével, N. Daum, M. Schneider, *Nanotechnology* **2011**, *22*, 275103/1–275103/7; c) Y. L. Xu, J. Sherwood, Y. Qin, D. Crowley, M. Bonizzoni, Y. P. Bao, *Nanoscale* **2014**, *6*, 1515–1524.
[17] T. A. C. Kennedy, J. L. MacLean, J. W. Liu, *Chem. Commun.* **2012**, *48*, 6845–6847.
[18] a) N. Schaeffer, B. Tan, C. Dickinson, M. J. Rosseinsky, A. Laromaine, D. W. McComb, M. M. Stevens, Y. Q. Wang, L. Petit, C. Barentin, D. G. Spiller, A. I. Cooper, R. Levy, *Chem. Commun.* **2008**, *34*, 3986–3988; b) B. Santiago González, M. J. Rodríguez, C. Blanco, J. Rivas, M. A. Lopez-Quintela, J. M. Gaspar Martinho, *Nano Lett.* **2010**, *10*, 4217–4221; c) G. H. Yang, J. J. Shi, S. Wang, W. W. Xiong, L. P. Jiang, C. Burda, J. J. Zhu, *Chem. Commun.* **2013**, *49*, 10757–10759.
[19] a) J. Zheng, J. T. Petty, R. M. Dickson, *J. Am. Chem. Soc.* **2003**, *125*, 7780–7781; b) W. I. Lee, Y. Bae, A. J. Bard, *J. Am. Chem. Soc.* **2004**, *126*, 8358–8359.
[20] A. Lopez, J. W. Liu, *J. Phys. Chem. C* **2013**, *117*, 3653–3661.
[21] a) X. Yang, M. M. Shi, R. J. Zhou, X. Q. Chen, H. Z. Chen, *Nanoscale* **2011**, *3*, 2596–2601; b) P. P. Bian, J. Zhou, Y. Y. Liu, Z. F. Ma, *Nanoscale* **2013**, *5*, 6161–6166.
[22] a) W. B. Chen, X. J. Tu, X. Q. Guo, *Chem. Commun.* **2009**, *45*, 1736–1738; b) T. T. Chen, Y. H. Hu, Y. Cen, X. Chu, Y. Lu, *J. Am. Chem. Soc.* **2013**, *135*, 11595–11602.
[23] V. Venkatesh, A. Shukla, S. Sivakumar, S. Verma, *ACS Appl. Mater. Interfaces* **2014**, *6*, 2185–2191.
[24] J. Chen, Q. F. Zhang, T. A. Bonaccorso, P. G. Williard, L. S. Wang, *J. Am. Chem. Soc.* **2014**, *136*, 92–95.
[25] a) M. Brust, M. Walker, D. Bethell, D. J. Schiffrin, R. Whyman, *J. Chem. Soc., Chem. Commun.* **1994**, 801–802; b) J. F. Hicks, A. C. Templeton, S. W. Chen, K. M. Sheran, R. Jasti, R. W. Murray, *Anal. Chem.* **1999**, *71*, 3703–3711; c) J. Sun, J. Zhang, Y. D. Jin, *J. Mater. Chem. C* **2013**, *1*, 138–143.
[26] Q. Mu, H. Xu, Y. Li, S. J. Ma, X. H. Zhong, *Analyst* **2014**, *139*, 93–98.
[27] a) E. Lonn, S. Yusuf, M. J. Arnold, P. Sheridan, J. Pogue, M. Micks, M. J. McQueen, J. Probstfield, G. Fodor, C. Held, J. J. Genest, *N. Engl. J. Med.* **2006**, *354*, 1567–1577; b) K. H. Bønaa, I. Njølstad, P. M. Ueland, H. Schirmer, A. Tverdal, T. Steigen, H. Wang, J. E. Nordrehaug, E. Arnesen, K. Rasmussen, *N. Engl. J. Med.* **2006**, *354*, 1578–1588.
[28] a) J. B. van Meurs, R. A. Dhonukshe-Rutten, S. M. Pluijm, M. van der Klift, R. de Jonge, J. Lindemans, L. C. de Groot, A. Hofman, J. C. Witteman, J. P. van Leeuwen, M. M. Breteler, P. Lips, H. A. Pols, A. G. Uitterlinden, *N. Engl. J. Med.* **2004**, *350*, 2033–2041; b) R. R. McLean, P. F. Jacques, J. Selhub, K. L. Tucker, E. J. Samelson, K. E. Broe, M. T. Hannan, L. A. Cupples, D. P. Kiel, *N. Engl. J. Med.* **2004**, *350*, 2042–2049.
[29] N. Nagano, M. Ota, K. Nishikawa, *FEBS Lett.* **1999**, *458*, 69–71.
[30] Z. K. Wu, R. C. Jin, *Nano Lett.* **2010**, *10*, 2568–2673.
[31] Z. Z. Huang, F. Pu, Y. H. Lin, J. S. Ren, X. G. Qu, *Chem. Commun.* **2011**, *47*, 3487–3489.
[32] a) H. Xu, M. Hepel, *Anal. Chem.* **2011**, *83*, 813–819; b) R. Peng, L. Lin, X. Wu, X. Liu, X. Feng, *J. Org. Chem.* **2013**, *78*, 11602–11605.
[33] a) M. Zhang, M. X. Yu, F. Y. Li, M. W. Zhu, M. Y. Li, Y. H. Gao, L. Li, Z. Q. Liu, J. P. Zhang, D. Q. Zhang, T. Yi, C. H. Huang, *J. Am. Chem. Soc.* **2007**, *129*, 10322–10323; b) B. Tang, Y. L. Xing, P. Li, N. Zhang, F. B. Yu, G. W. Yang, *J. Am. Chem. Soc.* **2007**, *129*, 11666–11667; c) J. H. Lee, C. S. Lim, Y. S. Tian, J. H. Han, B. R. Cho, *J. Am. Chem. Soc.* **2010**, *132*, 1216–1217; d) M. H. Lee, J. H. Han, P. S. Kwon, S. Bhuniya, J. Y. Kim, J. L. Sessler, C. Kang, J. S. Kim. *J. Am. Chem. Soc.* **2012**, *134*, 1316–1322.
[34] a) X. M. Guan, B. Hoffman, C. Dwivedi, D. P. Matthees, *J. Pharm. Biomed. Anal.* **2003**, *31*, 251–261; b) I. A. Cotgreave, P. Moldéus, *J. Biochem. Biophys. Methods* **1986**, *13*, 231–249.
[35] a) R. Hong, G. Han, J. M. Fernández, B. J. Kim, N. S. Forbes, V. M. Rotello, *J. Am. Chem. Soc.* **2006**, *128*, 1078–1079; b) S. S. M. Hassan, G. A. Rechnitz, *Anal. Chem.* **1982**, *54*, 1972–1976.

Received: June 8, 2014
Revised: July 14, 2014
Published online: August 11, 2014

